Molecular dynamics simulations on devitrification: The PbF 2 case

Maurício A. P. Silva, André Monteil, Younès Messaddeq, and Sidney J. L. Ribeiro

Citation: The Journal of Chemical Physics **117**, 5366 (2002); doi: 10.1063/1.1501119
View online: http://dx.doi.org/10.1063/1.1501119
View Table of Contents: http://scitation.aip.org/content/aip/journal/jcp/117/11?ver=pdfcov
Published by the AIP Publishing

Molecular dynamics simulations on devitrification: The PbF_2 case

Maurício A. P. Silva[a] and André Monteil
POMA UMR CNRS 6136, Université d'Angers, 2 bd. Lavosier, 49045 Angers, France

Younès Messaddeq and Sidney J. L.Ribeiro
Instituto de Química-UNESP, CP.355, CEP 14801-970, Araraquara, SP, Brazil

(Received 16 April 2002; accepted 24 June 2002)

In this work molecular dynamics simulations were performed to reproduce the kinetic and thermodynamic transformations occurring during melt crystallization, vitrification, and glass crystallization (devitrification) of PbF_2. Two potential parameters were analyzed in order to access the possibility of modeling these properties. These interionic potentials are models developed to describe specific characteristic of PbF_2, and thermodynamic properties were well reproduced by one of them, while the other proved well adapted to simulate the crystalline structure of this fluoride. By a modeled nonisothermal heat treatment of the glass, it was shown that the devitrification of a cubic structure in which the Pb–Pb distances are in good agreement with theory and experiment. © *2002 American Institute of Physics.* [DOI: 10.1063/1.1501119]

I. INTRODUCTION

In the last years a new class of oxyfluoride glass has appeared as an important composite aiming at the development of new photonic devices. These mixed systems, composed by a well-known glass former oxide, like SiO_2, B_2O_3, TeO_2, or GeO_2 and heavy metal fluorides, can be obtained in the glassy state by the conventional melting/quenching technique, at room atmosphere.[1–5] In addition to the relatively simple preparation method and optical characteristics of rare earth doped samples, very interesting devitrification (glass crystallization) features are presented by these systems. For example, the $MO–PbF_2–CdF_2$ systems ($MO=SiO_2$, B_2O_3, and GeO_2) are characterized by the devitrification of a cubic structure, identified as lead fluoride β-PbF_2, with the possibility of obtaining transparent glass ceramics under controlled thermal treatments. $Cd_{1-x}Pb_xF_2$-type solid solutions were also identified in some devitrified samples.[2]

The crystallization processes in glasses have been studied by various generations of glass researchers. The knowledge of the nucleation and crystal growth processes has always been the goal of these scientists due to its importance, in the beginning, to avoid glass crystallization and, nowadays, to control it. Experimental techniques employed in this kind of research are mainly thermal analysis differential scanning calorimetry/differential thermal analysis (DSC/DTA), but other techniques have been employed, for example, x-ray diffraction, vibrational spectroscopy (IR, Raman) and x-ray absorption spectroscopy (XANES/EXAFS).

On the other hand, molecular modeling has been used extensively as a power tool in the determination of structures of glasses, mainly silicates and fluorozirconates. The interest in these deterministic and stochastic methods has grown with the computational development but, although the utilization of these modeling techniques to understand the devitrification processes can be helpful, few works[6] have been published concerning the thermodynamic changes in glasses, during devitrification, modeled by computational methods like molecular dynamics.

Our goal in this paper is to optimize the numerical conditions of modeling the devitrification processes of an inorganic material, using the molecular dynamics (MD) technique. Our experience in the crystallization behavior of oxyfluoride glasses led us to investigate the devitrification process of a ''fictive'' PbF_2 glass, aiming at the study of the glass–ceramic formation in fluorosilicate glasses.

II. INTERIONIC POTENTIALS

In MD simulations, it is important to keep in mind that the interionic potentials used are models trying to describe a specific characteristic of a material. For example, a potential can be developed to well describe the structural characteristics of a material, in detriment of a good reproduction of its dynamic properties. That is the case, for example, of the usual potentials employed to describe the structure of silica glasses, in which the structural characteristics are well simulated, whereas the glass transition temperature is obtained in a higher value than the one observed experimentally.[7]

The literature concerning MD simulations of PbF_2 is not extensive. We have selected two works to investigate, due to their interesting similarities and differences. Walker *et al.*[8] have studied the conduction behavior of PbF_2, which presents a diffuse transition from a nonconducting to a fast-ion (superionic) conducting state at about 700 K. Another work involving PbF_2 was made by Hayakawa *et al.*,[9] in a structural study of $PbF_2–PbO–SiO_2$ glasses. It was proposed that ions Pb^{2+} and F^- are present as clusters Pb–F along the Si–O chains, and the glassy network former/modifier features of Pb^{2+} and F^- ions depend on the PbO/SiO_2 ratio.

The short-range atomic interaction used in both papers can be described by the Buckingham potential, which consists of a repulsive exponential and an attractive dispersion term between the pairs (represented by $-C/r^6$)

[a]Electronic mail: mauricio.silva@univ-angers.fr

TABLE I. Buckingham two-body pair potentials used in MD simulations of PbF_2.

	Walker *et al.*[a]			Hayakawa *et al.*[b]		
Atomic pair	A(eV)	ρ(Å)	C(eV Å^6)	A(eV)	ρ(Å)	C(eV Å^6)
Pb–Pb	0.0	0.0	0.0	2.51×10^6	0.170	3.10×10^{-2}
Pb–F	122.7	0.516	0.0	1.36×10^6	0.170	3.10×10^{-2}
F–F	10 225	0.225	107.3	7.31×10^5	0.170	4.29×10^{-2}

[a]Reference 8.
[b]Reference 9.

$$U(r)=Z_iZ_je^2/r_{ij}+A_{ij}\exp(-r_{ij}/\rho_{ij})-C/r_{ij}^6, \quad (1)$$

where Z is the charge on ions of species i and j, in units of the electronic charge e, and r_{ij} is the distance between these ions. A_{ij} is the short-range coefficient for repulsion and ρ_{ij} is an adjustable constant. Although the interionic potentials used in the works cited above were the same, the pair potential parameters used in the MD simulations were rather different, as listed in Table I. These two sets of pair potential parameters will hereafter be called the ''Walker model'' and ''Hayakawa model.''

As our interest in this work is to model the transformations during vitrification/devitrification of PbF_2, we are dealing with thermodynamic and structural properties. In this case, an ideal interionic potential is the one that has the better compromise between these properties. This paper is divided in the following way: We have investigated the two potential parameters cited above by means of radial distribution function analysis, $g(r)$, simulation of EXAFS spectra using modeled configurations, and ion diffusion coefficient analysis (Secs. III and IV). This preliminary investigation allowed us to select the potential parameters that better correspond to our goals and in Sec. V we will present our results obtained with the modeling of the vitrification and devitrification processes of PbF_2. Finally, the presented results will be discussed in Sec. VI and the conclusions traced in Sec. VII.

III. MOLECULAR DYNAMICS CALCULATIONS AND EXAFS SIMULATIONS

For the long-range electrostatics (Coulomb) potentials the Ewald sum technique[10] was used.

The simulations were performed using the DL_POLY program, developed in the CCLRC Daresbury Laboratory.[11] For the generation of the crystal structure, we have constructed a cubic fcc structure, of lattice constant $a=5.93$ Å, containing 768 atoms (256 cations and 512 anions) in a cubic box, duplicated in the three directions to infinity (periodic boundary condition). For the two sets of parameters (Walker and Hayakawa), the simulation procedures were identical. The system was equilibrated at 300 K in the canonical (NVT) ensemble during a run of 20 000 steps, with time step fixed at 0.001 ps, and then relaxed at the same time interval (20 ps) in the microcanonical (NVE) ensemble. Then, as the experimental x-ray absorption spectra were obtained at liquid nitrogen temperature, the system was cooled down to 77 K and the processes of equilibration and relaxation done under the same conditions. Finally, a 5000-steps (5 ps) run in the NVE ensemble was performed in order to record the radial distribution functions, $g(r)$.

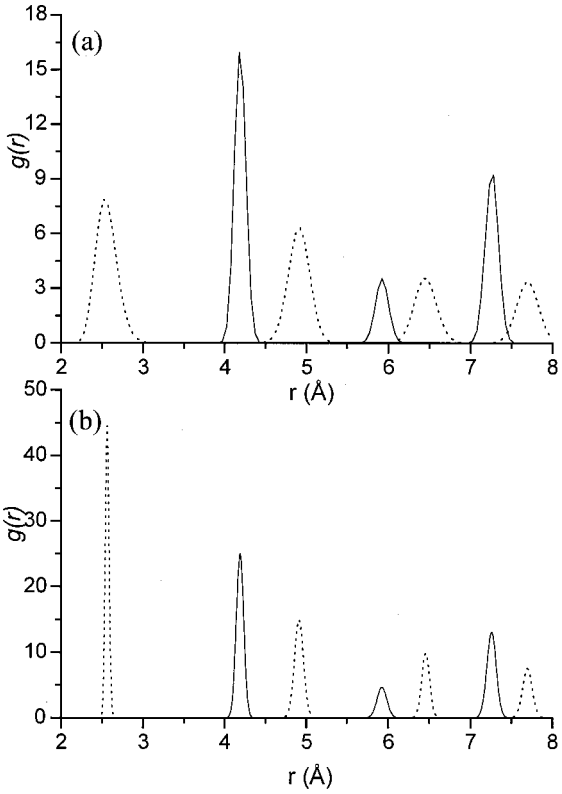

FIG. 1. Radial distribution functions $g(r)$ for the pairs Pb–Pb (solid line) and Pb–F (dotted line), obtained by MD simulations using the Walker (a) and Hayakawa (b) models.

The Pb L_{III}-edge EXAFS spectra simulations were performed using the FEFF8.1 program.[12] The modeled configurations were introduced in the ATOMS field and a configuration average over all absorbers (Pb) atoms was considered using the CFAVERAGE card, in order to consider eventual distortion in the absorbing atoms surroundings. The EXAFS spectra Fourier transforms were obtained using Michalowicz's EXAFS98 program.[13] ''Modeled'' EXAFS spectra were compared with experimental ones whose conditions for sample preparation, spectra acquisition, and data analysis were detailed in a previous work.[2]

IV. COMPARISON BETWEEN MODELS

Figures 1(a) and 1(b) show the $g(r)$ curves for the Pb–Pb and Pb–F pairs obtained by the Walker and Hayakawa models, respectively, and Table II compares the coordination numbers and interatomic distances obtained from the MD simulations and the theoretical values, calculated for a perfect fcc PbF_2 crystal of cell parameter $a=5.93$ Å. The coordination numbers and interatomic distances are related to a central Pb atom. From Fig. 1 one can observe narrower and more intense peaks obtained with the Hayakawa model than those from the Walker model. Also, from Table II, one

TABLE II. Kind of coordination atom and interatomic distances from a central Pb atom simulated using the Walker and Hayakawa models, compared to theoretical values calculated considering a perfect fcc PbF_2 crystal of cell parameter $a=5.93$ Å.

Theoretical	Walker model	Hayakawa model
8 F at 2.57 Å	8 F at 2.55 Å	8 F at 2.57 Å
12 Pb at 4.19 Å	12 Pb at 4.17 Å	12 Pb at 4.19 Å
24 F at 4.91 Å	24 F at 4.91 Å	24 F at 4.91 Å
6 Pb at 5.93 Å	6 Pb at 5.93 Å	6 Pb at 5.93 Å
24 F at 6.46 Å	24 F at 6.45 Å	24 F at 6.46 Å
24 Pb at 7.26 Å	24 Pb at 7.26 Å	24 Pb at 7.26 Å
32 F at 7.70 Å	32 F at 7.70 Å	32 F at 7.70 Å

observes that the interatomic distance are best reproduced, mainly in the first coordination shells, by the Hayakawa model.

Figures 2(a) and 2(c) shows the comparison between the Pb L_{III}-edge EXAFS spectrum of a cubic β-PbF_2 sample, obtained experimentally at 77 K (open circles), the modeled spectra, calculated by the FEFF8.1 program using as atomic configuration the DM simulation using the Walker (a) and Hayakawa (c) models (solid circles) and the EXAFS signal calculated by the FEFF8.1 program with the ''perfect'' fcc structure of β-PbF_2 generated by the ATOMS program[14] (solid line). The ATOMS program generates the atomic coordinates for a given crystal from its crystallographic parameters. For a better visualization of the contribution of each coordination shell to the whole signal, a Fourier transforamtion was performed in these spectra, using a Kaiser window ($\tau=2.5$) between 3.48 and 16.00 $Å^{-1}$; they are illustrated for the Walker and Hayakawa models, in Figs. 2(b) and 2(d), respectively.

While Fig. 2(a) shows a relatively good agreement between the EXAFS oscillations of the modeled structure and those obtained experimentally, Fig. 2(b) reveals an important characteristic presented by the potentials of the Walker model. The first coordination shell, formed by fluorine atoms around the central lead atom, presents a weaker intensity accompanied by an asymmetry in the modeled signal, in

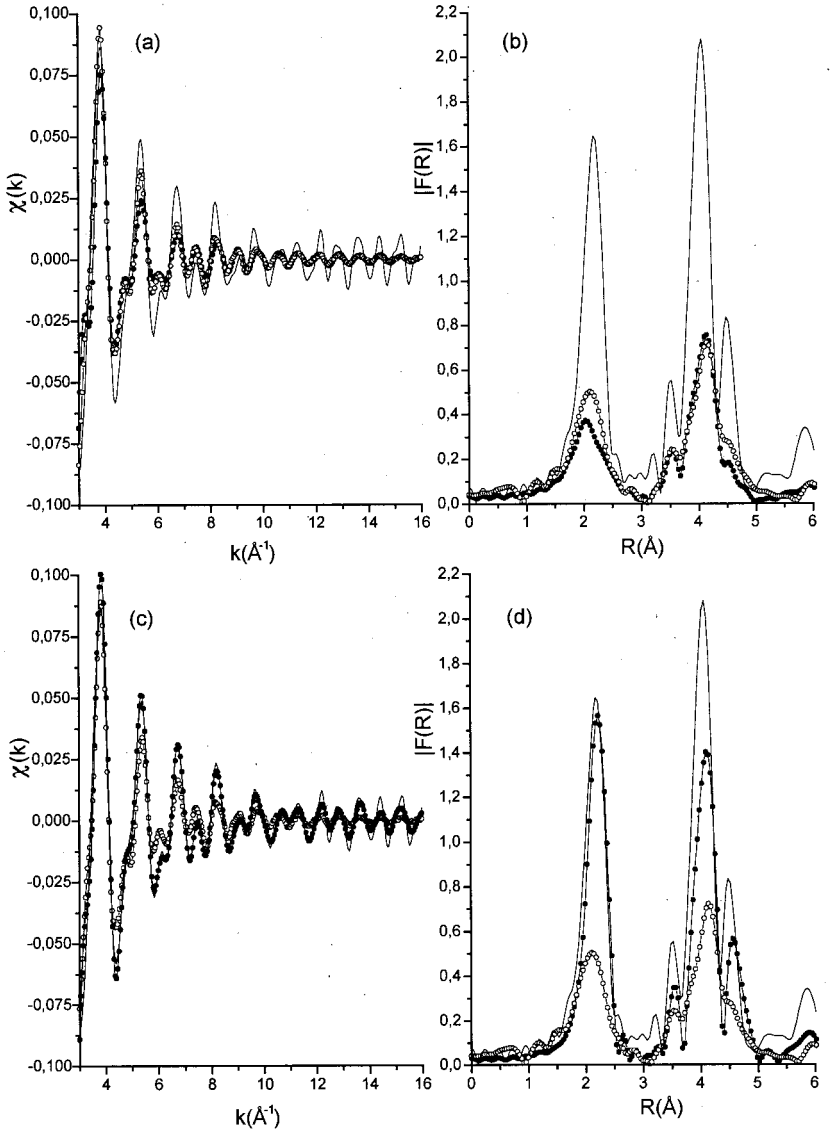

FIG. 2. β-PbF_2 L_{III}-edge EXAFS spectra, $\chi(k)$, and respective Fourier transformed signals, $|F(R)|$ (Kaiser window between 3.48 and 16.00 $Å^{-1}$), obtained experimentally (open circles) and calculated ones using the MD configurations (solid circles) and the perfect fcc structure given by the ATOMS program (solid line). (a) and (b): MD results from the Walker model; (c) and (d): MD results from the Hayakawa model.

comparison to the experimental signal. In the same way, the modeled signal at the right side of the peak corresponding to the second coordination shell is less intense than the experimental one. These results reflect the anionic disorder present in the modeled configuration.

The comparison made in Fig. 2(c) show that the modeled EXAFS oscillations obtained with the Hayakawa model are more intense than those obtained experimentally. On the other hand, a good agreement is obtained when one compares the modeled signal with the perfect crystal EXAFS oscillations, calculated by FEFFF8.1 AND ATOMS. In Fig. 2(d) the differences between the experimental and calculated (using ATOMS or MD configurations) data are noteworthy, indicating the highly ordered environments obtained in the calculated EXAFS spectra. Comparing both calculated Fourier-transformed EXAFS signals in Fig. 2(d), one can observe a difference in the intensity of the main peak at about 4 Å, relative to the Pb–Pb and Pb–F interactions in the second lead coordination shell. This can suggest some degree of disorder obtained by the model proposed by Hayakawa, in relation to the perfect ordering produced by ATOMS. But, compared with the experimental signal, the differences between both calculated signals are rather irrelevant.

The other method employed to compare the features of the two models was to follow the approximate ion diffusion coefficient during constant heating. This study allows us to determine the possibility of a qualitative reproduction of thermodynamic characteristics of PbF_2, such as crystal melting and the transition from the state of low conduction to that of fast-ion conduction. The parameters suggested by Walker *et al.* were obtained to describe the ionic disorder of PbF_2 at high temperature, and it was proposed[8] that the simulation results are in good agreement with the experiment. On the other hand, concerning the parameters suggested by Hayakawa *et al.*,[9] obtained to well reproduce the structure of a lead oxyfluorosilicate glass, no information about the possibility of reproduction of phase transformations was available. In order to investigate it, we have performed simulations with both models, in which a constant heating was employed, from 300 to 3500 K, with equilibration and relaxation (20 ps) processes for various temperatures. Figures 3(a) and 3(b) illustrate the curves of variation of Pb^{2+} (circles) and F^- (squares) diffusion coefficients, D, with temperature, obtained with the models of Walker and Hayakawa, respectively.

Figure 3(a) reveals the occurrence of two transformations, labeled 1 and 2. Transformation 1 occurs at about 700 K in the fluorine D curve and is related to the transition from the state of low conduction to that of fast-anion conduction (superionic state). This result shows a very good agreement with experimental value presented in the literature.[15,16] Transformation 2, which occurs in both Pb^{2+} and F^- D curves at 2000 K, reflects the melting temperature. This phase transformation, better observed in the Pb^{2+} D curve, occurs at a higher temperature than the one observed experimentally, $T_m \approx 1100$ K.[17]

The thermodynamic properties discussed above are not reproduced efficiently by the Hayakawa model, as seen in Fig. 3(b). This figure indicates that the increase of mobility

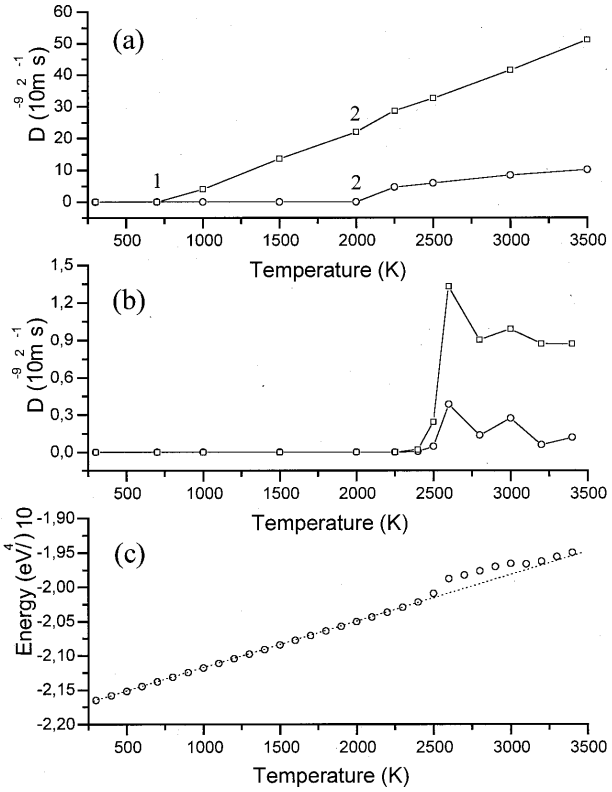

FIG. 3. (a) and (b): Diffusion coefficient variation with temperature of F^- (squares) and Pb^{2+} (circles) ions obtained by MD simulations using the Walker model and the Hayakawa model, respectively. (c) Internal energy variation during heating simulation using the Hayakawa model (the dotted line is a guide to the eyes). Phase transitions: (1) nonconducting to a fast-ion (superionic) conducting state; (2) melting.

of both ions occurs simultaneously, during fusion, at about 2500 K. After the jump of the diffusion coefficient values, with rising temperature, there is a nonconventional diminution of the ions' mobility. This after-melting behavior is also observed in Fig. 3(c), which illustrates energy variation during heating. At about 2500 K one observes the fusion clearly, characterized by the endothermic discontinuity (change in the specific heat during solid–liquid transition), but, with rising temperature, the system relaxes into a lower energy state. These physically senseless behaviors are not explained and are probably due to mathematical artifacts of the potential used.

As recalled in the beginning of this paper, the interionic potentials used in MD simulations are models trying to describe, with more or less success, a *specific* characteristic of a material. As seen from the results presented, the interionic potential parameters proposed by Hayakawa *et al.*[9] reproduce very successfully the structural characteristics of a perfect crystalline fcc PbF_2 and, as shown in the cited reference, it is a good potential to describe the structure of oxyfluorosilicate glasses. But, it does not reproduce the thermodynamic transformations during heat. On the other hand, the interionic potential parameters proposed by Walker *et al.*,[8] while showing an excessive anionic structural disorder in the crystal phase, even at low temperature, are a good model to describe the transformations concerning our work: the kinetics of vitrification and thermodynamics of devitrification of

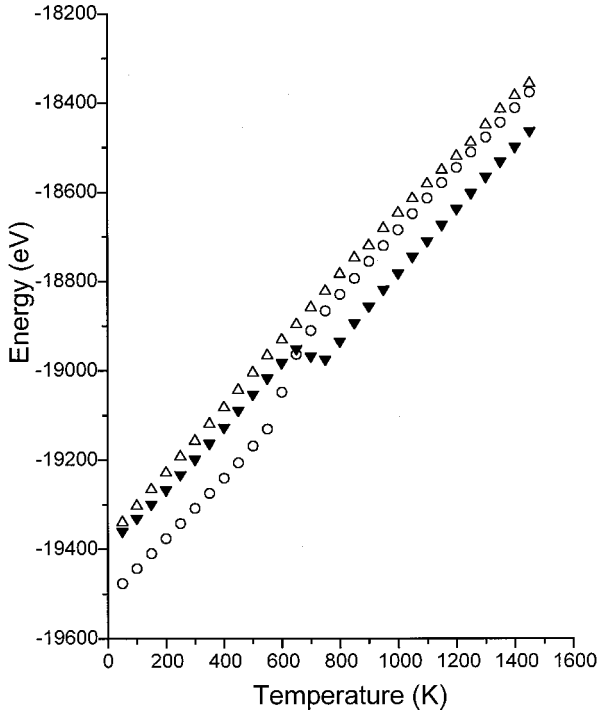

FIG. 4. Evolution of the internal energy with temperature during the cooling and heating processes simulated using the Walker model. Circles: slow (1 Kps^{-1}) cooling process; up, open triangles: fast (100 Kps^{-1}) cooling process; down, closed triangles; glass heating process (1.5K ps^{-1}).

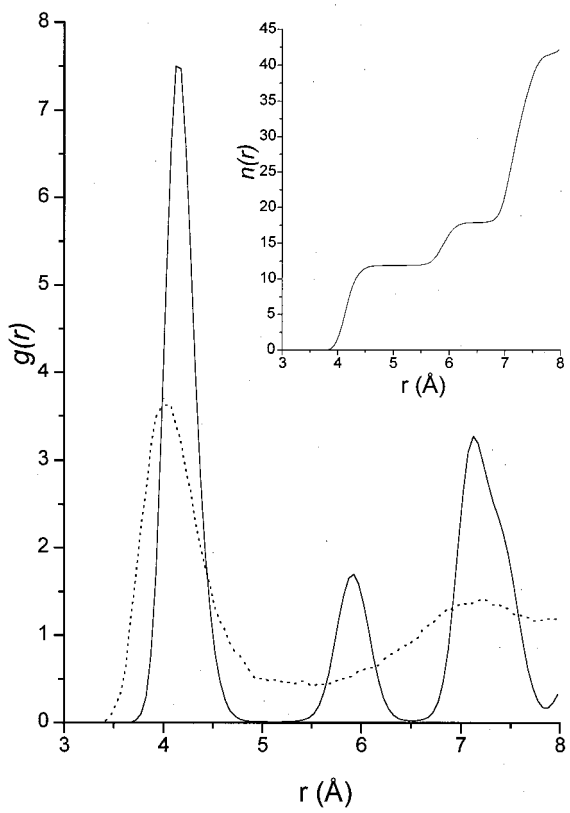

FIG. 5. Radial distribution functions, $g(r)$, of the Pb–Pb pairs at 200 K, recorded for the configurations obtained after slow (1 Kps^{-1}, solid line) and fast (100 Kps^{-1}, dotted line) cooling processes. Inset: cumulated distribution function, $n(r)$, obtained after slow cooling process indicating the Pb–Pb coordination numbers as 12, 6, and 24, respectively, as expected for a fcc structure.

PbF_2. The results presented hereafter are those obtained by MD simulation using the Walker model.

V. CRYSTALLIZATION FROM THE MELT/ VITRIFICATION/DEVITRIFICATION MODELING

The MD simulations on phase transformations were made with 2592 atoms (864 cations and 1728 anions), as the periodic boundary condition, used to avoid the effects of artificial boundaries, would harm the dynamics in smaller systems.[6] Our interest here is to reproduce the melt crystallization, with a slow cooling rate, and the glass formation, with a fast cooling rate. Then, by heating the amorphous phase, one would expect the relaxation (stabilization) of the glassy structure, promoting the glass crystallization (devitrification). In this way, simulations were performed in the following steps: starting from the liquid phase (3000 K), the system was cooled down to 50 K with cooling rates of 1 and 100 Kps^{-1}. One would expect the melt crystallization during the slow-cooling process, while an amorphous phase is expected to be obtained from the fast-cooling regime. The glassy PbF_2 was then heated up to 1500 K at a rate of 1.5 Kps^{-1} in order to verify the devitrification process.

Figure 4 shows the evolution of the internal energy with temperature during the cooling and heating processes, where circles and up, open triangles denote the slow and fast cooling cases, respectively, and down, closed triangles denote the glass heating process.

During the melt slow-cooling process (circles), the drop at about 650 K in the internal energy curve reveals the occurrence of an exothermic transformation. This transformation corresponds to the melt crystallization, as revealed in Fig. 5, which shows the $g(r)$ curves of the Pb–Pb pairs at 200 K, recorded for the configurations obtained after slow (solid line) and fast (dotted line) cooling processes. The $g(r)$ curve for the fast-cooling case shows an amorphous-like structure, while the one obtained after the slow-cooling rate indicates the formation of a regular Pb–Pb structure, at about the same intercationic distances and coordination numbers obtained for the crystal [see Fig. 1(a) and Table II]. The inset in Fig. 5 represents the cumulated distribution function, $n(r)$, which indicates the number of atoms in each coordination shell. These values are in good agreement with the expected values.

Finally, as expected, glass crystallization was obtained by heating, indicated by the exothermic transformation occurring in the corresponding internal energy curve (down, closed triangles) in Fig. 4 at about 650 K. This result is confirmed by Fig. 6, which shows the $g(r)$ curves for the Pb–Pb pairs at 600 K (dotted line) and 800 K (solid line), obtained during heating the glass at 1.5 Kps^{-1}. No crystal-like structure is observed in the $g(r)$ curve at 600 K but, at 800 K one observers the occurrence of the crystallization process, revealed by the structures at about 4.2, 5.9, and 7.3 Å. The $n(r)$ curve in the inset of Fig. 6 reveals the expected coordination numbers for a fcc structure.

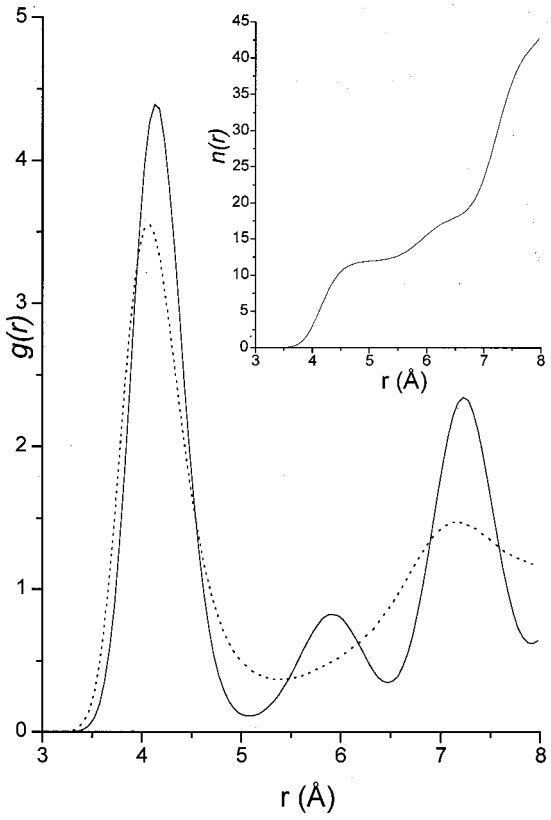

FIG. 6. $g(r)$ curves for the Pb–Pb pairs at 600 K (dotted line) and 800 K (solid line), obtained during heating the glass at 1.5 Kps^{-1}. Inset: $n(r)$ curve indicating the expected value sof cation–cation coordination numbers for a fcc structure.

VI. DISCUSSION

As stated in this paper, the first part of our study was dedicated to investigating two parameter potentials used to describe the interatomic interaction forces in PbF_2, proposed by Walker *et al.*[8] and Hayakawa *et al.*[9] Our goals were to evaluate the characteristics best described by these two models, in order to use them in our study of phase transformations occurring during fusion, quenching, and reheating a PbF_2 modeled sample.

The calculation of Pb L_{III}-edge EXAFS spectra using, as atomic configurations, the modeled structures given by Walker and Hayakawa models has been successfully employed to determinate the structural characteristic simulated by these models. As seen in Figs. 2(a) and 2(b), related to the Walker model, by comparing the modeled EXAFS spectra with the experimental one, a difference in the oscillations in the $\chi(k)$ spectra and peak's width and intensity in the Fourier transformed EXAFS signal is observed. The discrepancies, better visualized in Fig. 2(b), mainly in the intensity of the peak relative to the first Pb coordination shell and the discordance in the right side of the peak related to the second coordination shell, reflect an excessive anionic disorder in the modeled structure. This feature is also observed in Fig. 1, where the peaks in the radial distribution function curves appear as a broader distribution (but centered at expected positions) in relation to the ones in the Hayakawa model case. In fact, the Walker model parameters were developed for studies on disorder anomalies in PbF_2, caused by anion diffusion and defects, and reveal a good accordance of this characteristic with experiment. Nevertheless, though this model favors the modeling of ion transport features, also verified in this work [Fig. 3(a)], it does not reproduce perfectly the experimental crystal anionic structure.

On the other hand, the EXAFS spectrum calculated using the atomic configuration obtained by MD simulation with the Hayakawa model is in good agreement with the one calculated using an atomic configuration obtained by the ATOMS program. Nevertheless, no structural or thermal disorder was considered during calculations using ATOMS (Debye–Waller factor $\sigma=0$) and its structure can be considered as a crystallographically perfect β-PbF_2 crystal, free of defects and thermal agitation. This observation explains the higher intensity of the modeled EXAFS oscillations in relation to the experimental ones, which presents, naturally, a non-negligible Debye–Waller factor ($\sigma>0$). These results, added to the narrower peaks and better distance distributions observed in the $g(r)$ curves obtained by the Hayakawa model [Figs. 1(a) and 1(b)] lead to the conclusion that this model is more adapted to the reproduction of the crystalline structure of β-PbF_2 than the Walker model. Nevertheless, it was seen that the Hayakawa model does not reproduce successfully the ion conclusion characteristics [Fig. 3(b)] and thermodynamic features like crystal fusion [Fig. 3(c)]. These properties present a nonconventional behavior of stabilization after fusion which is physically senseless.

On the other hand, the Walker model is well adapted to describe the effects of fluorine mobility anomalies during heating [Fig. 3(a)], with a transition temperature obtained from MD simulations ($T_t=700$ K), close to the ones observed experimentally [$T_t\approx700$ K (Ref. 15), or $T_t\approx711$ K (Ref. 16)]. These mobility anomalies are related to the superionic conduction characteristics of PbF_2. Its high conductivity properties are connected to the strong disordering in the fluorine sublattice, caused by thermal generation of Frenkel defects, inducting anionic transport.[15] On the other hand, the cation sublattice, as exemplified for $Cd_{1-x}Pb_xF_2$ mixed crystals,[18,19] plays an important role in the fluorine disordering process. It has been proposed that the lower Pb–F interaction coefficient compared to the other fluorides is responsible for the superionic properties of PbF_2.

The modeling of kinetic and thermodynamic properties using the Walker parameters was successful. The same calculations shown here for the Walker model were carried out with the Hayakawa model, but without success. Glass crystallization was attained by modeling the glass heating. A mean distance of about 4.2 Å between two closer lead atoms was obtained, as seen in Fig. 6. This result is in total agreement with Pb L_{III}-edge EXAFS analysis in SiO_2–PbF_2–CdF_2 glass ceramics[2] (in which the crystalline phase is the β–PbF_2), $R_{Pb-Pb}=4.20$ Å. Moreover, in the first cation–cation vicinity, as expected for a fcc structure, the coordination of 12 lead atoms was obtained, which corroborates the occurrence of the crystallization process.

Of course, the modeled crystallization can be controlled and crystal growth obtained by an isothermal run at the be-

ginning of the crystallization temperature, T_x, at about 700 K for a more or less long time period, depending on the proportion of crystalline phase desired.

VII. CONCLUSIONS

The main goal of this work was to reproduce, by MD simulations, the kinetic and thermodynamic transformations occurring during melt crystallization, vitrification, and glass crystallization (devitrification) of an inorganic material such as PbF_2, as it is the main crystalline phase present in oxyfluoride glass ceramics, important composite material with applications in photonics. Two potential parameters, the Walker and Hayakawa models, were analyzed in order to access the possibility of modeling these properties. The Hayakawa model revealed an excellent potential parameter to describe the crystalline structure of cubic β-PbF_2, but did not reproduce successfully the phase transformations of interest in this work. The Walker model generates a good cationic structure but the anionic disordering is more important than the one observed experimentally, as shown by the EXAFS spectrum simulation. On the other hand, anion diffusion and crystal melting are relatively well reproduced by this model. With this model it was also possible to reproduce the liquid–solid phase transition, during slow cooling of the melt as well as the vitrification of the material by fast cooling. Moreover, by a modeled nonisothermal heat treatment of the glass, it was possible to obtain the devitrification of a cubic structure in which the Pb–Pb distances are in good agreement with theory and experiment. Finally, it was proposed that an isothermal treatment near T_x can control the amount of crystalline phase in the glass.

ACKNOWLEDGMENTS

The authors thank Valérie Briois (from the French synchrotron laboratory, LURE) for experimental support during EXAFS data acquisitions. This work is supported by CAPES (Brazil) and the Conseil Régional des Pays de la Loire (France).

[1] G. H. Beall and L. R. Pinckney, J. Am. Ceram. Soc. **82**(1), 5 (1999).
[2] M. A. P. Silva, S. J. L. Ribeiro, Y. Messaddeq, V. Briois, and M. Poulain, J. Phys. Chem. Solids (in press).
[3] M. A. P. Silva, S. J. L. Ribeiro, Y. Messaddeq, V. Briois, and M. Poulain, J. Braz. Chem. Soc. **13**(2), 200 (2002).
[4] M. A. P. Silva, M. Poulain, F. Villain, V. Briois, S. J. L. Ribeiro, and Y. Messaddeq, J. Phys. Chem. Solids **62**, 1055 (2001).
[5] L. A. Bueno, P. Melnikov, Y. Messaddeq, and S. J. L. Ribeiro, J. Non-Cryst. Solids **247**, 87 (1999).
[6] M. Shimono and H. Onodera, Mater. Sci. Eng. A **304–306**, 515 (2001).
[7] K. Vollmayr, W. Knob, and K. Binder, Phys. Rev. B **54**(22), 15808 (1996).
[8] A. B. Walker, M. Dixon, and M. J. Gillan, J. Phys. C **15**, 4061 (1982).
[9] S. Hayakawa, A. Osaka, H. Nishioka, S. Matsumoto, and Y. Miura, J. Non-Cryst. Solids **272**, 103 (2000).
[10] M. P. Allen and D. J. Tildesley, *Computer Simulation of Liquids* (Clarendon, Oxford, 1989).
[11] DL_POLY *is a package of molecular simulation routines written by W. Smith and T. R. Forester, copyright The Council for the Central Laboratory of the Research Councils, Daresbury Laboratory at Daresbury, Nr. Warrington* (1996).
[12] A. L. Ankudinov, B. Ravel, J. J. Rehr, and S. D. Conradson, Phys. Rev. B **58**, 7565 (1998).
[13] A. Michalowicz, *EXAFS pour le Mac (Societé Française de Chimie, Paris*, 1991), p. 102.
[14] B. Ravel, J. Synchrotron Radiat. **8**, 314 (2001).
[15] I. Kosacki and K. Zalibowski, Phys. Status Solidi A **108**, 765 (1988).
[16] W. Schröter and J. Nölting, J. Physique Coll. 41 C6 s. 7C20-3 (1980).
[17] C. E. Derrington and M. O'Keeffe, Nature (London) **246**, 44 (1973).
[18] I. Kosacki, Appl. Phys. A: Solids Surf. **49**, 413 (1989).
[19] M. A. P. Silva, S. J. L. Ribeiro, Y. Messaddeq, V. Briois, F. Villain, and M. Poulain, Solid State Ionics **147**, 135 (2002).